pp 971–983. © Royal Aeronautical Society 2016
doi: 10.1017/aer.2016.39

The generation of tonal noise from sawtooth trailing-edge serrations at low Reynolds numbers

D. J. Moreau
d.moreau@unsw.edu.au

C. J. Doolan
School of Mechanical and Manufacturing Engineering
University of New South Wales
Sydney
Australia

ABSTRACT

The flow and noise created by sawtooth trailing-edge serrations has been studied experimentally at a low Reynolds number. Experiments have been performed on a flat-plate model with an elliptical leading edge and an asymmetrically bevelled trailing edge at Reynolds numbers of $\mathrm{Re}_c = 1 \times 10^5$–$1.3 \times 10^5$, based on chord. Wide serrations with a wavelength (λ_s) to amplitude ($2h$) ratio of $\lambda_s/h = 0.6$ were found to reduce the overall sound pressure level by up to 11 dB. In contrast, narrower serrations with $\lambda_s/h = 0.2$ produce tonal noise and increase the overall noise level by up to 4 dB. Intense vortices across the span of the trailing edge with narrow serrations are shown to be the source of tonal noise. Wide serrations reduce turbulent velocity fluctuations at low frequencies which explains the lower radiated noise. The narrow serrations that produce low Reynolds number tonal noise were shown previously to be effective at higher Reynolds numbers ($\mathrm{Re}_c > 2 \times 10^5$), demonstrating that care is needed to fully understand the flow field over serrations for all intended operating conditions.

Keywords: Aeroacoustics; trailing-edge noise; wind tunnel testing; aerofoil noise

Received 10 December 2012; revised 1 October 2015; accepted 29 October 2015.

1.0 INTRODUCTION

An increasing number of engineering applications employ lifting surfaces that operate at relatively low aerofoil chord Reynolds numbers ($Re_c < 5 \times 10^5$), such as micro wind turbines, unmanned aerial vehicles and underwater control surfaces. In these applications, trailing-edge noise produced by the scattering of boundary-layer vorticity at the sharp trailing edge[1,2], is a dominant noise mechanism. Various passive trailing-edge modifications such as porous edges[3,4], brush- or comb-type extensions[5,6] and trailing-edge serrations have been investigated as a means of reducing trailing-edge noise. This paper focuses on aerofoil self-noise reduction using sawtooth trailing-edge serrations and in particular, at low Reynolds number ($Re_c \leq 1.3 \times 10^5$).

Several theoretical[7,8], numerical[9] and experimental[10-19] studies have shown that trailing-edge serrations are a valid means of aerofoil self-noise reduction. Howe[7,8] derived an analytical noise radiation model for a flat-plate serrated trailing edge in low Mach number flow. Howe's theory states that the noise reduction achieved with trailing-edge serrations is related to a reduction in the effective span-wise length of the trailing edge that contributes to noise generation and that the level of attenuation achieved is dependent on the frequency of sound and the serration geometry.

Most of the experimental studies on trailing-edge serrations have examined their effect on full-scale wind turbine blades or wind-tunnel scale aerofoil models at high Reynolds numbers ($Re_c > 5 \times 10^5$, based on chord)[10-16]. These studies have reported that trailing-edge serrations reduce broadband noise levels by up to 7 dB at low frequencies and produce a high-frequency noise increase of approximately 2 dB above approximately 1 kHz. Gruber et al[13] performed a detailed parametric study of 36 different sawtooth serrated edges to determine how serration geometry influences broadband noise reduction. Trailing-edge serrations were found to be an efficient means of noise reduction for $h/\delta > 0.5$ and reach a maximum efficiency when $h/\delta > 2$, where $2h$ is the serration root-to-tip amplitude and δ is the trailing-edge boundary-layer thickness. The noise reduction was also found to improve with decreasing serration wavelength.

Chong et al[18,19] were some of the few to investigate the capability of trailing-edge serrations in reducing aerofoil self-noise at low Reynolds numbers of $1 \times 10^5 < Re_c < 5 \times 10^5$. They observed that, in this Reynolds number range, the noise produced by the base flow (a NACA 0012 aerofoil with straight trailing edge) contained a broadband contribution and a number of high-amplitude tonal components. Trailing-edge serrations were found to inhibit flow separation close to the trailing edge, and in turn, reduce the amplitude of the broadband and tonal noise components.

Previous studies have shown that trailing-edge serrations can reduce aerodynamic noise, although not as much as Howe's[7,8] theory would suggest. Possibly, this is due to the breakdown of Howe's assumption that the serrations do not affect the turbulence passing the edge, although this is yet to be proven. Also, there are limited studies concerning the effect of serrations at low Reynolds numbers, and in particular, for cases where the base flow (i.e. no serrations) produces broadband noise. In this paper, the effect of serrations on noise generated by a flat-plate model operating at a low Reynolds number ($Re_c = 1 \times 10^5$–1.3×10^5) is presented. The results show how noise can be reduced or increased through the creation of tones depending on the serration geometry. An explanation is provided in terms of the velocity field close to the serrations, indicating that the serrations create a form of vortex shedding. The results are important, as they show that there is a strong link between the serrations and the flow field, and that this coupling is more

https://doi.org/10.1017/aer.2016.39 Published online by Cambridge University Press

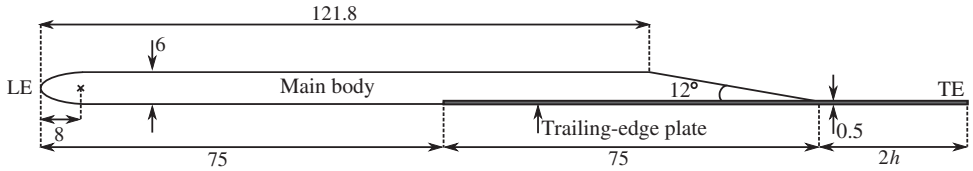

Figure 1. Schematic diagram of the flat-plate model. Dimensions in mm and $2h = 15$ and 30 mm for the straight and serrated trailing edges, respectively.

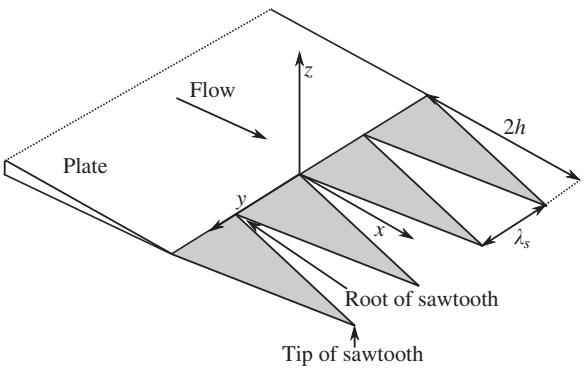

Figure 2. Sawtooth serrations at the trailing edge of a flat plate with root-to-tip amplitude of $2h$ and wavelength of λ.

significant than the effect of the serrations on the efficiency of noise production at the edge.

2.0 EXPERIMENTAL SET-UP

2.1 Test model

The flat-plate model is composed of a main steel body and a detachable trailing-edge plate made from brushed aluminum, as shown in Fig. 1. The main body has a span of $s = 450$ mm and a thickness of $h_t = 6$ mm. The Leading Edge (LE) of the main body is elliptical, with a semi-major axis of 8 mm and a semi-minor axis of 3 mm, while the Trailing Edge (TE) is asymmetrically bevelled at an angle of 12°. Three 0.5 mm-thick trailing-edge plates were used (one at a time): one with a straight, unserrated configuration and two with serrations. The flat-plate model with the straight, unserrated trailing edge is used as the reference configuration for all tests and so will be referred to as the reference plate, hereafter. Two different serration geometries are compared in this study, both with root-to-tip amplitude of $2h = 30$ mm: one with a wavelength of $\lambda_s = 3$ mm ($\lambda_s/h = 0.2$, termed *narrow serrations*) and the other with $\lambda_s = 9$ mm ($\lambda_s/h = 0.6$, termed *wide serrations*). The two geometrical parametres h and λ_s are defined in Fig. 2. Figure 3 shows the trailing-edge plates and the flat-plate model with wide serrations attached to the contraction. As shown in Fig. 3(b), the root of the serrations is aligned with the trailing edge of the main body so that only the serrated component of the trailing-edge plate is exposed to the flow. The area of the reference plate is equivalent to that

https://doi.org/10.1017/aer.2016.39 Published online by Cambridge University Press

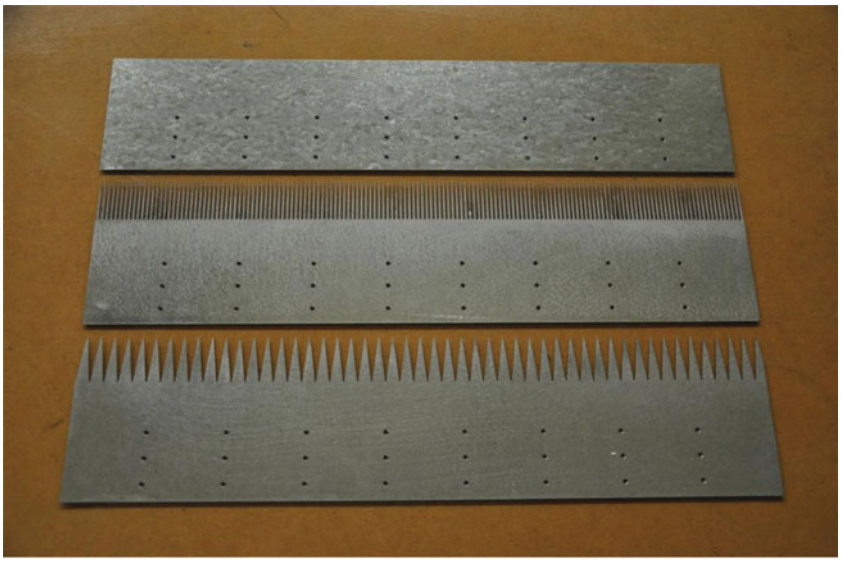

(a) Trailing edge plates. Top: straight unserrated trailing edge (reference), middle: narrow serrations with $\lambda = 3$ mm, bottom: wide serrations with $\lambda = 9$ mm.

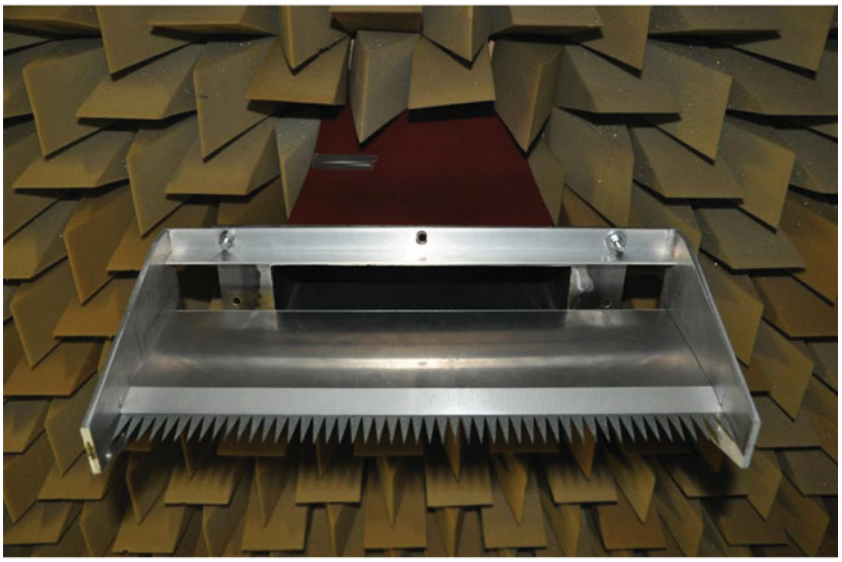

(b) The flat plate model with wide trailing edge serrations held between the side plates and attached to the contraction outlet.

Figure 3. (Colour online) The trailing-edge plates and the flat-plate model in situ.

of the flat plate with serrated trailing edges giving the same effective wetted surface area in all three test cases. The serrated- and reference-plate models all have the same mean chord of $c = 165$ mm.

The trailing-edge plate is fastened to the main body with 24 M2 $\times$ 0.4 screws. These screws protruded slightly (<0.4 mm) into the flow below the lower flat surface of the plate

https://doi.org/10.1017/aer.2016.39 Published online by Cambridge University Press

model; however, this was consistent for all three plate configurations. Hot-wire measurements within the boundary layer on the lower flat surface of the plate, downstream of the screws, confirmed that any flow disturbances created at the screws dissipated well before the trailing edge. The method of trailing-edge attachment used in this study avoids bluntness at the root of the serrations that may produce vortex shedding and a tonal noise component. The flat-plate model was then held between two side plates and attached to the contraction at zero angle-of-attack, as shown in Fig. 3(b).

Figure 3(b) shows the span of the flat-plate models extends beyond the width of the contraction outlet. This was done to eliminate the noise produced by the interaction of the side-plate boundary layers with the model leading edge. To determine the influence of this mounting method on radiated noise, the acoustic spectra of two different reference-plate models (with straight trailing edge) have been previously compared by the authors[20]. One plate had a span equal to the width of the contraction outlet (275 mm) and was held between two side plates that were aligned with the contraction edges. The second plate had a span of 450 mm, as shown in Fig. 3. The noise radiated by the two plates was found to be highly comparable over the entire frequency range of interest from 250 Hz to 10 kHz.

2.2 Anechoic wind-tunnel facility

Experiments were performed in an anechoic wind tunnel located at the University of Adelaide[21]. The anechoic wind-tunnel test chamber is 1.4 m × 1.4 m × 1.6 m (internal dimensions) and has walls that are acoustically treated with foam wedges, providing a near reflection-free environment above 250 Hz. The facility contains a contraction outlet that is rectangular in cross-section with dimensions of 75 mm × 275 mm. The maximum-flow velocity of the free jet is approximately 40 m/s and the free-stream turbulence intensity at the contraction outlet is 0.33%[22]. In this study, experiments were conducted at free-stream velocities between $U_\infty = 9$ and 12 m/s corresponding to Reynolds numbers $\mathrm{Re}_c = 1 \times 10^5$ and 1.3×10^5, respectively.

2.3 Measurement techniques

Acoustic measurements were recorded at a single-observer location using a B&K 1/2" microphone (Model No. 4190), located 554 mm directly below the trailing edge of the reference plate. Hot-wire anemometry was used to obtain unsteady velocity data in the wake of the serrated- and reference-plate models. A TSI 1210-T1.5 single-wire probe with wire length of $L = 1.27$ mm and a wire diameter of $d = 3.81$ μm was used in experiments. The sensor was connected to a TSI IFA300 constant temperature anemometer system and positioned using a Dantec automatic traverse with 6.25 μm positional accuracy. The traverse allowed continuous movement in the stream-wise (x), span-wise (y) and vertical (z) directions. The co-ordinate system used in this study is shown in Fig. 2 and is located at centre span at the root of the trailing-edge serrations. Acoustic and flow data were recorded for each flat-plate model using a National Instruments PCI-4472 board at a sampling frequency of 5×10^4 Hz for a sample time of 8 s and 4 s, respectively. Data are presented in narrowband format with a frequency resolution of 2 Hz and have been calculated using Welch's averaged modified periodogram method of spectral estimation with a Hamming window function and 75% overlap. The 95% confidence interval[23] on the narrow-band power density is –0.79/+0.85 dB/Hz for the acoustic measurements and $-1.4 \times 10^{-6}/+8.0 \times 10^{-6}$ m^2/s

https://doi.org/10.1017/aer.2016.39 Published online by Cambridge University Press

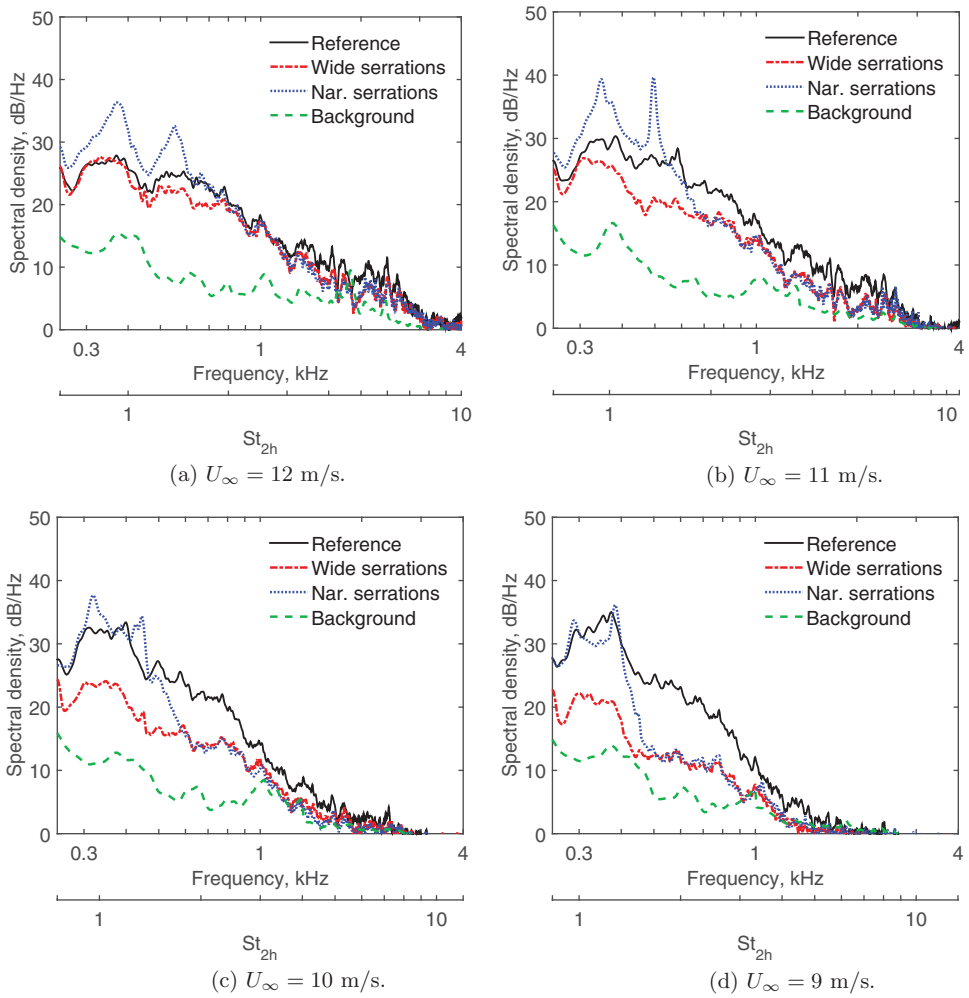

Figure 4. (Colour online) Far-field acoustic spectra for the reference plate and the plates with trailing-edge serrations at $U_\infty = 9$ to 12 m/s. The background spectra indicate the tunnel noise level without the plate present.

for the velocity measurements. Additionally, the error in the mean velocity estimates is 0.32%.

3.0 EXPERIMENTAL RESULTS

3.1 Acoustic measurements

Figure 4 shows acoustic spectra for the reference plate and the plates with trailing-edge serrations at flow speeds of $U_\infty = 9$ to 12 ms^{-1}. The background noise spectra which indicate the tunnel noise levels without the plate present are also shown in this figure for comparison. The spectra in Fig. 4 have been plotted with the x-axis indicating both frequency in kHz and Strouhal number, St_{2h}, based on serration root-to-tip amplitude, $2h$. While noise spectra are

https://doi.org/10.1017/aer.2016.39 Published online by Cambridge University Press

Table 1
Reduction in overall sound pressure levels between 250 Hz and 4 kHz with the trailing-edge serrations.

U_∞, m/s	Wide serrations, dB	Narrow serrations, dB
12	1.4	−4.1
11	4.4	−4.1
10	8.0	−1.0
9	10.9	1.8

presented at a single-observer location only, trailing-edge serrations have not been found to modify the directivity of the noise radiated by a straight trailing edge[17].

Figure 4 shows that the noise produced by the reference plate at all flow speeds is broadband in nature. The low-frequency noise levels of the reference plate (below 500 Hz) are observed to increase in amplitude with decreasing flow speed.

The wide serrations are shown in Fig. 4 to produce broadband noise levels and a low-frequency region of attenuation that increases in amplitude with decreasing flow speed. A reduction of up to 16 dB is achieved in the narrowband noise levels with the wide serrations (see Fig. 4(d)). The low-frequency region of noise attenuation is bounded by a Strouhal number based on serration root-to-tip amplitude, $2h$, of $St_{2h} = 6.4$. Table 1 states the reduction in overall sound pressure level between 250 Hz and 4 kHz, achieved with trailing-edge serrations at flow speeds between $U_\infty = 9$ and 12 m/s. This table shows that the wide serrations reduce the overall sound pressure level by up to 11 dB.

The far-field noise spectra in Fig. 4 show that the narrow serrations produce regions of increased acoustic amplitude with two distinct tones. The narrow serrations increase the narrow-band noise levels by up to 14 dB (see Fig. 4(b)) and produce an increase in the overall sound pressure level at flow speeds between $U_\infty = 10$ and 12 m/s, as shown in Table 1. The two tones produced by the narrow serrations occur at a constant Strouhal number of $St_{2h} = 1$ and 1.3. Above a Strouhal number of $St_{2h} \approx 2$, the narrow serrations are shown to perform similarly to the wide serrations.

The authors have previously examined the effect of trailing-edge serrations on a flat plate at higher flow speeds of $U_\infty = 15$ to 38 m/s[17], using the same experimental set-up and flat-plate models as in this study. Figure 5 shows the narrow-band far-field acoustic spectra for the reference plate and the two plates with trailing-edge serrations at flow speeds of $U_\infty = 15$ and 38 m/s. The background noise spectra are also shown in this figure for comparison. At flow speeds of $U_\infty = 15$ m/s and above, both the narrow and wide, serrated trailing edges produce broadband noise and achieve reductions of up to 13 dB in the narrow-band noise levels (in the high-frequency region between 5 and 10 kHz at $U_\infty = 38$ m/s and between 1.5 and 4.5 kHz at $U_\infty = 15$ m/s). Trailing-edge serrations that are effective at reducing noise at higher Reynolds numbers may, therefore, produce undesirable tonal noise during low Reynolds number operation.

3.2 Velocity measurements

The normalised mean (U/U_∞) velocity profiles measured in the very near wake of the reference plate and the two plates with trailing-edge serrations at free-stream velocities

https://doi.org/10.1017/aer.2016.39 Published online by Cambridge University Press

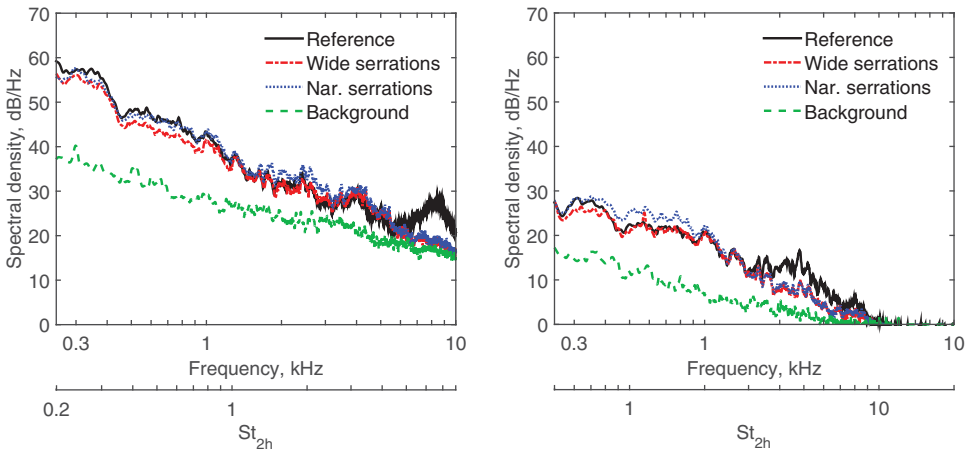

(a) $U_\infty = 38$ m/s. (b) $U_\infty = 15$ m/s.

Figure 5. (Colour online) Far-field acoustic spectra for the reference plate and the plates with trailing-edge serrations at $U_\infty = 15$ and 38 m/s. The background spectra indicate the tunnel noise level without the plate present.

between $U_\infty = 9$ and 12 m/s are shown in Fig. 6. The profiles for the reference plate have been measured at $x/c = 0.1$, which corresponds to 1 mm downstream of the straight trailing edge, while for the two plates with trailing-edge serrations, the profiles have been measured at $x/c = 0.19$, which corresponds to 1 mm downstream of the tip of a serrated tooth.

At each flow speed, the velocity profiles for the three trailing-edge geometries in Fig. 6 differ significantly. This indicates that trailing-edge serrations alter the flow structure in the very near wake. The velocity profiles of each plate are qualitatively similar at flow speeds between $U_\infty = 9$ and 12 m/s, indicating that the same flow regimes are present at the trailing edge of each plate at all flow speeds.

The mean velocity profiles for the reference plate in Fig. 6 are highly asymmetric about the trailing edge. The mean velocity profiles for the reference plate at $U_\infty = 9$ and 12 m/s are compared with the Blasius solution[24] in Fig. 7. Below the trailing edge, the profiles are highly comparable to the theoretical Blasius profile, indicating that the flow is laminar throughout the boundary layer. On the top surface, the profiles display a more laminar inner region with significant deviation in the outer region of the boundary layer. This suggests that the laminar boundary layer separates at the bevel and then reattaches as a transitional boundary layer on the straight trailing-edge plate, just upstream of the trailing edge. The deviation in the outer boundary-layer region is associated with the growth of the separated shear layer over the bevel. The high levels of low-frequency noise observed for the reference plate in Fig. 4 are most likely due to eddies or flow perturbations in the transitional boundary layer on the top surface of the plate near the trailing edge. At lower flow speeds, the boundary layer will contain more spatially coherent eddies than at higher flow speeds, thus resulting in higher levels of low-frequency noise[25].

Figures 6 and 7 show the flat-plate boundary layer remains in a similar laminar-transitional state at flow speeds of 9 to 12 m/s. When the flow is in a laminar-transitional state, instabilities, known as Tollmien-Schlichting (T-S) waves, are present in the boundary layer. Sound is produced by the scattering of these boundary-layer instabilities at the trailing

https://doi.org/10.1017/aer.2016.39 Published online by Cambridge University Press

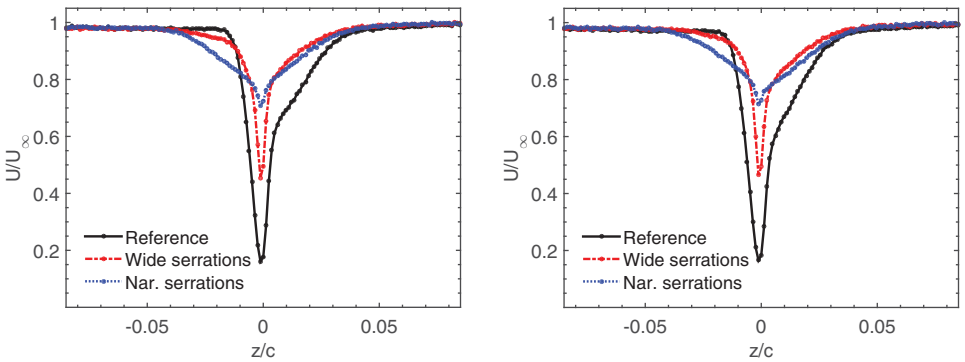

(a) $U_\infty = 12$ m/s. (b) $U_\infty = 11$ m/s.

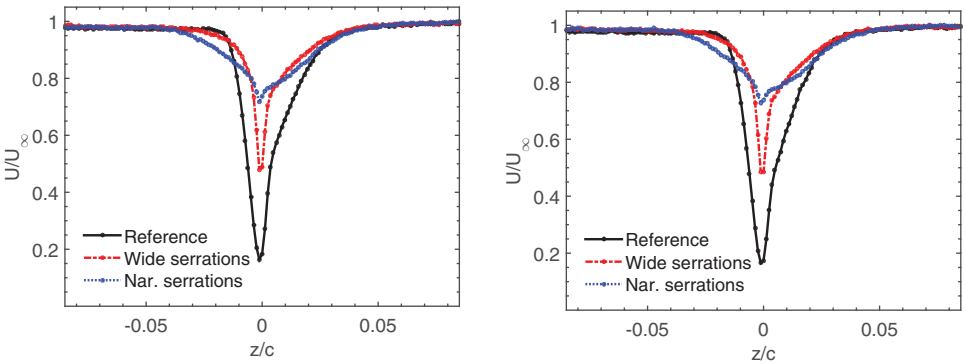

(c) $U_\infty = 10$ m/s. (d) $U_\infty = 9$ m/s.

Figure 6. (Colour online) Normalised mean velocity profiles at the trailing edge. The profiles for the reference plate have been measured at a position of $x/c = 0.1$, which corresponds to 1 mm downstream of the straight trailing edge. The profiles for the plates with trailing-edge serrations have been measured at the tip of a serrated tooth at a position of $x/c = 0.19$, which corresponds to 1 mm downstream of the serrated trailing edge.

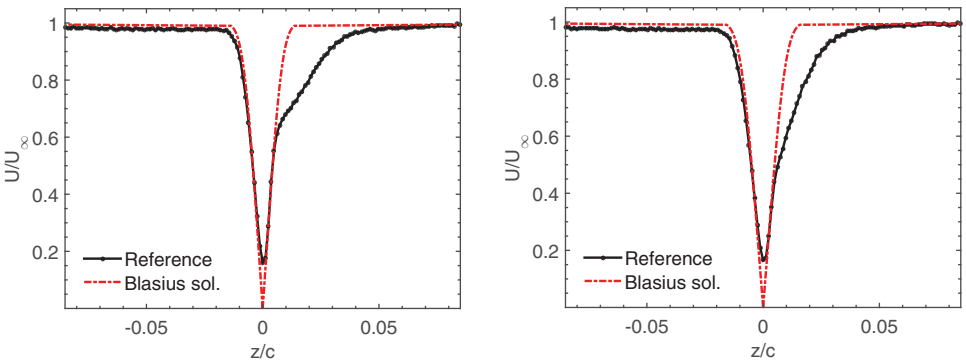

(a) $U_\infty = 12$ m/s. (b) $U_\infty = 9$ m/s.

Figure 7. (Colour online) Normalised mean velocity profiles at the trailing edge of the reference plate compared to the Blasius solution. The profiles for the reference plate have been measured at a position of $x/c = 0.1$, which corresponds to 1 mm downstream of the straight trailing edge.

https://doi.org/10.1017/aer.2016.39 Published online by Cambridge University Press

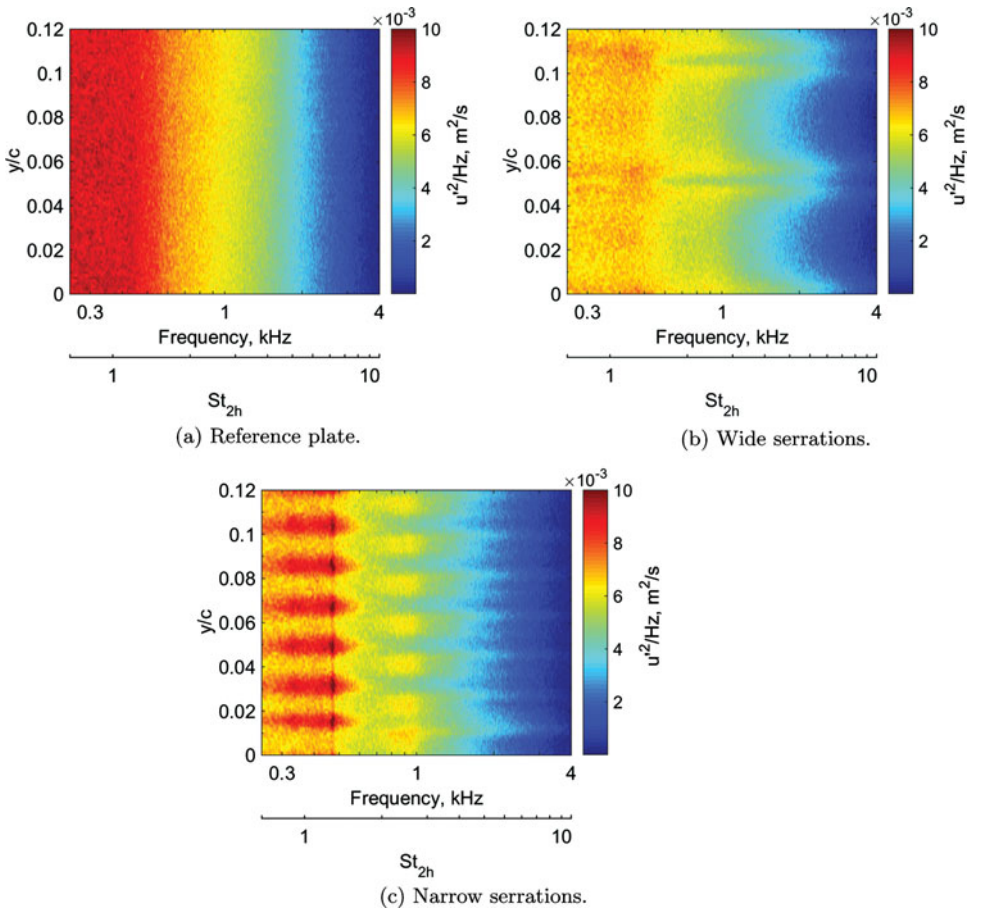

Figure 8. (Colour online) Velocity spectral maps measured in the span-wise (y) direction inline with the trailing edge at $U_\infty = 11$ m/s at a position of 1 mm downstream (at $x/c = 0.1$, $z/c = 0$ for the reference plate; and, at $x/c = 0.19$, $z/c = 0$ for the plates with trailing-edge serrations). In (b) and (c), a position of $y/c = 0$ corresponds to the tip of a serrated tooth.

edge[26-28]. The frequency distribution of T-S waves in the boundary layer is sensitive to small changes in Reynolds number, and for this reason, flow-speed variation is observed in the spectral shape and amplitude of the radiated noise in Fig. 4.

Figure 6 shows the wake of the plate with wide serrations is characterised by a slightly asymmetric velocity field. In comparison, the mean velocity profiles for the narrow serrations are largely symmetric about the trailing edge. Additionally, the profiles show the velocity deficit is more quickly recovered along the wake centerline for the plate with narrow serrations.

As the source of trailing-edge noise is the unsteady flow field about the trailing edge, time-varying flow data have been measured along the span in the near trailing-edge wake for each model. Velocity measurements are presented at the selected flow speed of $U_\infty = 11$ m/s only as the results are qualitatively similar at all flow speeds between $U_\infty = 9$ and 12 m/s.

Figure 8 shows spectral maps of the fluctuating velocity (u'^2/Hz) measured in the span-wise (y) direction along the trailing edge at a distance of 1 mm downstream from both the straight

https://doi.org/10.1017/aer.2016.39 Published online by Cambridge University Press

and serrated trailing edges. Figure 8(a) shows that the wake velocity field close to the trailing edge of the reference plate is comprised of broadband random velocity fluctuations across the span. High energy is observed at low frequencies, and this corresponds to the high levels of low-frequency trailing-edge noise shown in Fig. 4.

The spectral maps, measured in the near wake of the two plates with serrated trailing edges in Figs 8(b) and (c), show features that occur due to flow interaction with the serrations. These results also show that the trailing-edge serrations affect the flow field in the vicinity of the trailing edge, which is the source of the trailing-edge noise in Fig. 4.

The spectral maps for the flat plate with narrow serrations in Fig. 8(c) display high-intensity velocity fluctuations at the same frequencies as the two tones observed in the corresponding far-field noise spectrum (see Fig. 4(b)). The high-intensity velocity fluctuations at the tonal noise frequencies in the wake are attributed to vortex shedding from the tips of the serrated teeth. Figure 8(c) shows that the narrow serrations permit intense vortex shedding across the span, which results in the production of high-amplitude tonal noise. High energy fluctuations also exist in the space between the narrow, serrated teeth (e.g. at a frequency of 900 Hz or $St_{2h} = 2.6$ in Fig. 8(c)), which corresponds to the first harmonic of the second, higher-frequency tone in the far-field noise spectrum (see Fig. 4(b)). While no defined peak is observed at this frequency in the noise spectrum, a broad hump is visible at this frequency.

The spectral maps for the plate with wide serrations in Fig. 8(b) show weak vortex shedding also occurs from the tips of the wide serrations. This vortex-shedding process is low in amplitude and does not result in tonal noise production (see Fig. 4).

3.3 Discussion

At flow speeds of $U_\infty = 9$ to 12 m/s, both serration geometries are effective at reducing low-frequency noise between a Strouhal number of $St_{2h} = 1.4$ and 6.4 (see Fig. 4). The wide serrations outperform the narrow ones by achieving attenuation at all frequencies below $St_{2h} = 6.4$. The narrow serrations do not reduce noise below $St_{2h} = 1.4$, where it is intensified into two discrete tones at $St_{2h} = 1$ and 1.3.

The narrow serrations exhibit a symmetric wake profile (see Fig. 6), indicating that the boundary layers on the top and bottom surface of the trailing edge separate evenly and permit coherent vortex shedding in the wake. The narrow serrations have the same effect on the acoustic and flow field as the wide serrations at high frequencies ($St_{2h} \approx 2$), but vortex shedding occurs from the tips of the serrated teeth at low frequencies, resulting in high-amplitude acoustic tones (see Fig. 8(c)).

The wide serrations produce a slightly asymmetric wake profile (see Fig. 6), and correspondingly, weak vortex shedding occurs at the tips of the wide, serrated teeth (see Fig. 8(b)). The vortex shedding is low amplitude and does not result in tonal noise production. A low-frequency noise reduction is achieved with the wide serrations, as they reduce the low-frequency turbulence levels at the trailing edge (see Fig. 8(b)).

At flow speeds of $U_\infty = 15$ m/s and above, the tonal noise produced by the narrow serrations is suppressed and they produce broadband noise only (see Fig. 5). Figure 9 shows the normalised mean velocity profiles at the trailing edge of the plate with narrow serrations at flow speeds of $U_\infty = 12$ and 15 m/s. This figure shows that when the flow speed is increased to $U_\infty = 15$ m/s and the flow is more turbulent, the narrow serrations produce a highly asymmetric wake profile. Vortex shedding is suppressed in this case and only broadband noise production occurs.

https://doi.org/10.1017/aer.2016.39 Published online by Cambridge University Press

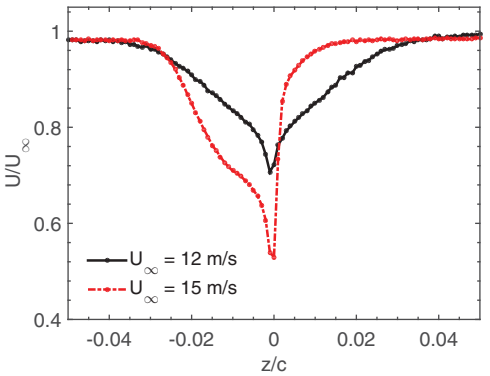

Figure 9. (Colour online) Normalised mean velocity profiles at the trailing edge of the plate with narrow serrations at $U_\infty = 12$ and 15 m/s. The profiles have been measured at the tip of a serrated tooth, at a position of $x/c = 0.19$, which corresponds to 1 mm downstream of the serrated trailing edge.

4.0 CONCLUSION

This paper has presented results of an experimental study on the effect of trailing-edge serrations on a flat plate at low Reynolds numbers. The wide trailing-edge serrations with wavelength to amplitude ratio of $\lambda_s/h = 0.6$ were found to reduce the overall sound pressure level by up to 11 dB. In contrast, the narrow trailing-edge serrations with $\lambda_s/h = 0.2$ produced high-amplitude tonal noise and an increase in the overall sound pressure level. Unsteady flow data in the near-trailing-edge wake showed that the narrow serrations permit the formation of intense vortices at each serration tip, resulting in the production of high-amplitude tonal noise, while the wide serrations reduce the turbulence at low frequencies resulting in an overall noise reduction.

The results show that serrations affect the flow structure at the trailing edge and that these changes are more important than any reduction in acoustic radiation efficiency. The results also have important practical implications. Serrations that are effective at a high Reynolds number may produce unwanted tones when operated at off-design conditions or during low Reynolds number operation. Thus, care is needed to fully understand the flow field over serrations for all intended operating conditions.

REFERENCES

1. BLAKE, W. Mechanics of flow induced sound and vibration, *Vol. II: Complex Flow-Structure Interactions*, 1986, Academic Press, New York, US.
2. BLAKE, W. and GERSHFELD, J. *Frontiers in Experimental Fluid Mechanics: The Aeroacoustics of Trailing Edges*, 1989, Springer-Verlag, Berlin.
3. HERR, M. and DOBRZYNSKI, W. Experimental investigations in low-noise trailing-edge design, *AIAA J*, 2005, **43**, (6), pp 1167-1175.
4. GEYER, T., SARRADJ, E. and Fritzsche, C. Measurement of the noise generation at the trailing edge of porous airfoils, *Experiments in Fluids*, 2010, **48**, pp 291-308.
5. HERR, M. On the design of silent trailing-edges, *New Results in Numerical and Experimental Fluid Mechanics VI*, 2008, **96**, pp 430-437.
6. FINEZ, A., JONDEAU, E., ROGER, M. and JACOB, M.C. Broadband noise reduction with trailing edge brushes, 16th AIAA Aeroacoustics Conference, 2010, AIAA Paper 2010-3980.

https://doi.org/10.1017/aer.2016.39 Published online by Cambridge University Press

7. HOWE, M.S. Aerodynamic noise of a serrated trailing edge, *J Fluids and Structures*, 1991, **5**, (1), pp 33-45.
8. HOWE, M.S. Noise produced by a sawtooth trailing edge, *J the Acoustical Society of America*, 1991, **90**, (1), pp 482-487.
9. SANDBERG, R.D. and JONES, L.E. Direct numerical simulations of low Reynolds number flow over airfoils with trailing-edge serrations, *J Sound and Vibration*, 2011, **330**, (16), pp 3818-3831.
10. BRAUN, K., VAN DER BORG, N., DASSEN, A., DOORENSPLEET, F., GORDNER, A., OCKER, J. and PARCHEN, R. Serrated trailing edge noise (STENO), European Wind Energy Conference, 1999, pp 180-183.
11. PARCHEN, R., HOFFMANS, W., GORDNER, Q., BRAUN, K., VAN DER BORG, N. and DASSEN, A. Reduction of airfoil self-noise at low Mach number with a serrated trailing edge, 6th International Congress on Sound and Vibration, 1999, pp 3433-3440.
12. OERLEMANS, S., FISHER, M., MAEDER, T. and KOGLER, K. Reduction of wind turbine noise using optimized airfoils and trailing-edge serrations, *AIAA J*, 2009, **47**, (6), pp 1470-1481.
13. GRUBER, M., JOSEPH, P.F. and CHONG, T.P. On the mechanisms of serrated airfoil trailing edge noise reduction, 17th AIAA/CEAS Aeroacoustics Conference, 2011, AIAA Paper 2011-2781.
14. CHONG, T.P., JOSEPH, P.F. and GRUBER, M. Airfoil self noise reduction by non-flat plate type trailing edge serrations, *Applied Acoustics*, 2013, **74**, (4), pp 607-613.
15. CHONG, T.P., VATHYLAKIS, A., JOSEPH, P.F. and GRUBER, M. Self-noise produced by an airfoil with nonflat plate trailing edge serrations, *AIAA J*, 2013, **51**, (10), pp 2665-2677.
16. FISCHER, A., BERTAGNOLIO, F., SHEN, W.Z., MADSEN, J., MADSEN, H.A., BAK, C., DEVENPORT, W. and INTARATEP, N. Wind tunnel test of trailing edge serrations for reduction of wind turbine noise, Inter–noise 2014, 2014, Paper 693.
17. MOREAU, D.J. and DOOLAN, C.J. Noise-reduction mechanism of a flat-plate serrated trailing edge, *AIAA J*, 2013, **51**, (10), pp 2513-2522.
18. CHONG, T.P., JOSEPH, P.F. and GRUBER, M. An experimental study of airfoil instability noise with trailing edge serrations, 16th AIAA/CEAS Aeroacoustics Conference, 2010, AIAA Paper 2010-3723.
19. CHONG, T.P., VATHYLAKIS, A., JOSEPH, P.F. and GRUBER, M. On the noise and wake flow of an airfoil with broken and serrated trailing edges, 17th AIAA/CEAS Aeroacoustics Conference, 2011, AIAA Paper 2011-2860.
20. MOREAU, D.J., DOOLAN, C.J., TETLOW, M., ROBERTS, M. and BROOKS, L.A. The flow and noise generated by a sharp trailing edge, The 17th Australasian Fluid Mechanics Conference, 2010, Paper 169.
21. LECLERCQ, D., DOOLAN, C. and REICHL, J. Development and validation of a small-scale anechoic wind tunnel, 14th International Congress on Sound and Vibration, 2007, Paper 105.
22. MOREAU, D.J., BROOKS, L.A. and DOOLAN, C.J. Broadband trailing edge noise from a sharp-edged strut, *J the Acoustical Society of America*, 2011, **129**, (5), pp 2820-2829.
23. BENDAT, J. and PIERSOL, A. *Random Data: Analysis and Measurement Procedures*, 2010, Wiley, New York, US.
24. CEBECI, T. and BRADSHAW, P. *Momentum Transfer in Boundary Layers*, 1977, Hemisphere Publishing Corporation, Washington, New York, US.
25. MOREAU, D.J., BROOKS, L.A. and DOOLAN, C.J. The effect of boundary layer type on trailing edge noise from sharp-edged flat plates at low-to-moderate Reynolds number, *J Sound and Vibration*, 2012, **331**, pp 3976-3988.
26. ARBEY, H. and BATAILLE, J. Noise generated by airfoil profiles placed in a uniform laminar flow, *JFluid Mechanics*, 1983, **134**, pp 33-47.
27. KINGAN, M.J. and PEARSE, J.R., Laminar boundary layer instability noise produced by an aerofoil, *J Sound and Vibration*, 2009, **322**, pp 808-828.
28. CHONG, T.P. and JOSEPH, P.F. Ladder structure in tonal noise generated by laminar flow around an airfoil, *J Acoustical Society of America*, 2012, **131**, pp 461-467.